

Oxidation characteristics of chars generated from wood impregnated with $(\text{NH}_4)_2\text{HPO}_4$ and $(\text{NH}_4)_2\text{SO}_4$

Carmen Branca, Colomba Di Blasi*

Dipartimento di Ingegneria Chimica, Università degli Studi di Napoli "Federico II", P.le V. Tecchio, 80125 Napoli, Italy

Received 9 November 2006; received in revised form 7 February 2007; accepted 12 February 2007

Available online 16 February 2007

Abstract

Thermogravimetric analysis (heating rates between 5 and 15 K/min up to 873 K) has been carried out in air of chars, generated from the pyrolysis of wood and wood impregnated with $(\text{NH}_4)_2\text{HPO}_4$ and $(\text{NH}_4)_2\text{SO}_4$ (5%, dry wood basis) which are widely used as flame retardants. Salts significantly alter the char reactivity, but a mechanism consisting of three parallel reactions always provides a good description of the measurements. The estimated activation energy and reaction order of the most important combustion reaction, which causes the release of about 71–80% of the volatile matter, are nearly the same for untreated and $(\text{NH}_4)_2\text{SO}_4$ impregnated samples (about 190–200 kJ/mol and 0.86). A lower activation energy (about 150 kJ/mol) and a higher reaction order (1.35) are obtained for $(\text{NH}_4)_2\text{HPO}_4$ treatments. Scanning electronic microscope (SEM) images show significant modifications in the morphological structure of both wood and char as a consequence of salt impregnation.
© 2007 Elsevier B.V. All rights reserved.

Keywords: Wood; Flame retardants; Char reactivity; Reaction mechanisms; Combustion

1. Introduction

Combustion processes of lignocellulosic fuels consist of pyrolysis with release of volatile species, producing flaming ignition and homogenous reactions in the gas phase, and smoldering and/or heterogeneous conversion of char [1]. The occurrence of the two stages can be simultaneous or sequential, depending on the size, geometry and properties of the burning item and the environment characteristics. In general, char reactivity is significantly affected by the nature of the solid fuel and the pyrolysis conditions which are responsible for pore structure, elemental composition, including the presence of inorganic matter, and aromaticity degree [2–5].

Oxidation kinetics and reactivity in air of char are important aspects for the development of comprehensive models for the description of fire hazards, where the oxidation of char controls the propagation of the smoldering front, or combustion plants based on renewable organic fuels and waste wood. Although, compared with fossil fuels, the studies on the oxidation kinetics of lignocellulosic chars are relatively a few, a significant level

of understanding has been reached [6–11]. Thermogravimetric curves in air of wood chars show a low-temperature shoulder (devolatilization) followed by a high-temperature peak (combustion) [9–10]. A n -order global reaction has been extensively used to model integral data but it provides a very poor description of the differential curves [10]. The combination with an additional first-order reaction for the devolatilization stage produces accurate predictions of both integral and differential curves and generally gives rise to much higher activation energies of the combustion reaction [10], which are comprised in the range of values reported for the low-temperature combustion of coal chars and graphite.

In reality, the use of wood products in institutional and commercial structures requires pre-treatments with flame retardants, which highly modify the yields and composition of the pyrolysis products and the characteristic temperatures and times of both solid pyrolysis and char combustion. In this way, the overall fire performances, evaluated in term of flame spread index, smoke index, etc. [12–14], are improved. It is also known that inorganic compounds, naturally present or added as flame retardants, may be neutral or act as inhibitors/enhancers of the smoldering reaction. In the case of cellulosic materials, it is noted [15] that some smolder inhibitors, such as ammonium salts and boric acid, also retard the glowing combustion of char,

* Corresponding author. Tel.: +39 081 7682232; fax: +39 081 2391800.
E-mail address: dibiasi@unina.it (C. Di Blasi).

although this is not a criterion for inhibition. Conversely, smolder enhancers, such as alkali or transition metal salts, also favor char combustion. However, detailed investigations about the combustion kinetics of chars derived from fire-retarded wood are not available.

In this study thermogravimetric measurements are presented of char produced from the pyrolysis of wood impregnated with diammonium phosphate ((NH₄)₂HPO₄, DAP) and diammonium sulfate ((NH₄)₂SO₄, DAS), two ammonium salts which are widely used as flame retardants [12–14]. A comparison with chars from untreated wood is also provided. Based on these results, a multi-step reaction mechanism is formulated and the related kinetic constants are estimated. Scanning electronic microscope (SEM) images are used to elucidate the differences between the char sample structures.

2. Materials and methods

The char samples investigated in this study were produced by means of a packed-bed reactor at a laboratory scale. Details about the pyrolysis process are already available elsewhere [16,17], so only the chief information is provided here. Nitrogen, fed through a jacket (internal diameter 0.089 m) at the reactor top, was heated by an electrical furnace and distributed by a perforated steel plate, which also supported the bed. The reaction zone was isothermal at a temperature of 800 K, the upper limit of primary wood decomposition without significant activity of secondary vapor-phase tar reactions, determined by a proper set point of the furnace. The sample (about 200 g sample) was placed in the feeder and, after nitrogen flushing and the attainment of the desired temperature, the feeding valve was opened, so that it was dropped inside the hot reactor and left there until complete conversion occurred. Wood particles (cubes 5 mm thick) were washed in hot (333 K) twice-distilled water (1 l for 100 g of wood) for 2 h and with stirring, which is an effective procedure to eliminate alkali compounds from ashes [18], thus avoiding their catalytic action on the conversion process. Washed and pre-dried samples were pyrolyzed to produce char samples to be used for comparison (in the following these samples are generally indicated as untreated). Impregnated samples were obtained by soaking 200 g of wood particles in DAP or DAS aqueous solution of 1 l of deionized water, added with the proper amount of salt, for 3 h. After drying, wood was weighted to evaluate the amount of salt adsorbed. A concentration of 5% for both salts in wood has been selected given that the numerous pyrolysis tests [17] indicated that dramatic changes in the yields and composition of production, and thus in reaction paths, had already occurred. Indeed, the yields of char increase from 23% (untreated wood) to 38 and 35% (total mass basis) for the treatments with DAP and DAS, respectively. The yields of water also increase (from about 18 to 37%), with a strong diminution in the amounts of organic condensable products, whereas the yields of permanent gases are barely affected. The pyrolysis temperature affects the yields of products and the volatile content of char [16]. However, it has been found that the reactivity of char in air is not significantly dependent on the final pyrolysis temperature for moderate values [7,10]. On the other hand, the heating rate during pyrolysis

is an important factor, but it cannot be easily controlled because, even for the same particle, it is a function of the position.

Prior to thermogravimetric tests, the char samples were milled to powder (particle sizes below 80 μm) and oven dried for 10 h at 373 K. The experimental system employed here is the same of previous studies for the kinetic analysis of solid fuels. It is a non-commercial system (precision 0.1 mg) and has already been described in detail (see, for instance, [8,10,19–21]). Extensive measurements (following, for instance, the methodology illustrated in [8]) show that, for an oxidative environment, the weight loss dynamics remain unaltered when the mass sample and/or the heating conditions are kept below certain limits. That is, the rate of weight loss (devolatilization or combustion) is always slower than the rate of mass transfer (convection/diffusion of volatile products and oxygen). Also, the temperature never exceeds the programmed evolution, given to the use of a PID controller, where the external heat flux is the manipulated variable, and a thin thermocouple in direct contact with the reacting sample. The attainment of negligible heat and mass transfer limitations is a necessary requisite for the subsequent kinetic analysis. Specifically, for the system applied here, the characteristic size of the process is the thickness of the sample layer. It has been observed that, for the samples under study, values up to 110 μm allow a good temperature control to be achieved, given maximum heating rates of 15 K/min and a final temperature of 873 K. These experimental conditions also ensure negligible spatial gradients of temperature and oxygen concentration. Hence, the tests have been made for sample layers about 100 μm thick, corresponding to a mass of 4 mg distributed over a surface 20 mm × 4 mm. Heating rates of 5, 10 and 15 K/min were applied in all cases. Each thermogravimetric test was made in triplicate, showing good reproducibility.

3. Kinetic mechanism

Following the kinetic model of wood char combustion presented in [10], a set of N independent parallel reactions, associated with lumped volatile species produced from the stages of devolatilization and combustion, is also proposed for the chars of interest here. The reactions rates present the usual Arrhenius dependence on temperature (A_i are the pre-exponential factors and E_i the activation energies) with a linear (devolatilization [22,23]) or a power law (combustion) dependence on the solid mass fraction, which can effectively take into account the evolution of the pore surface area during char combustion [7,10]. Since the sample temperature is a known function of time, the mathematical model consists of N ordinary differential equations for the mass fractions, Y_i , of the different lumped groups of volatile species whose initial values are indicated with v_i (stoichiometric coefficients).

The kinetic parameters are estimated through the numerical solution (implicit Euler method) of the mass conservation equations and the application of a direct method for the minimization of the objective function, which considers both integral (TG) and differential (DTG) data, following the method already described [20]. The simultaneous use of experimental data measured for several heating rates avoids possible compensation

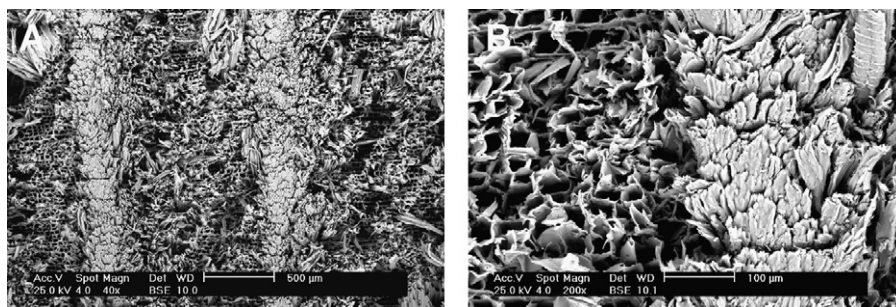


Fig. 1. SEM images of the cross (perpendicular to the trunk fibers) surface of untreated (washed) wood.

effects in the kinetic parameters [24]. The parameters to be estimated are the activation energies (E_1 – E_N), the pre-exponential factors (A_1 – A_N), the stoichiometric coefficients (ν_1 – ν_N) and the number of lumped classes of volatile species, N (a total of $3N + 1$ parameters). The optimization procedure has been executed by requiring the same values of the activation energies, pre-exponential factors and exponents for all the curves of each sample. In accordance with the usual procedure applied for the analysis of dynamic thermogravimetric data, the stoichiometric coefficients have been allowed to vary with the heating rates, because this parameter affects the dynamics of volatile release. From the practical point of view, given the relatively small range of heating rates examined, average values can be used.

4. Results

A description is provided first of the morphological structure of wood, after salt addition, and chars produced, using SEM images. Then results of kinetic modeling are presented including a comparison among the various samples.

4.1. Physical and morphological characteristics of the char samples

In general, heterogeneous reaction rates are affected by the morphological structure of the reacting char, that is, they generally comprise a chemical kinetic and a structural term. Among others, pore evolution is a function of the rate of release of volatiles, the amount of volatiles released and the inert material present in wood. Therefore, to gain information on the effects of salt addition on the morphological structure of the solid and thus on the oxidation rates, SEM images of the samples have been

made. Changes in the structure of wood, as a consequence of the two treatments, are shown by means of Fig. 1A and B (untreated washed wood), Fig. 2A and B (DAS treated wood) and Fig. 3A and B (DAP treated wood), which refer to the particle cross section (perpendicular to the wood trunk). Fig. 1A and B show the typical porous structure of wood with growing rings, which are in part swollen owing to hot water washing. The treatment with DAS contributes to producing a more ordered structure (Fig. 2A and B), probably cleaning part of the filaments and enlarging the macropore apertures, as already noted in the treatment with sulfuric acid [25]. DAS mainly appears as deposits along the lateral (parallel to the wood trunk) surfaces of the pores (not shown). The chief features introduced by the DAP treatment (Fig. 3A and B) consist in the significant salt deposits which partly occlude the pores of the wood structure and other apertures, especially in correspondence of the growing rings.

Char obtained from untreated (washed) samples preserves the main structural features of wood and the general morphological arrangement is not destroyed by the pyrolysis process. The release of volatile products gives rise to a honeycomb structure with pore enlargement (Fig. 4A and B, particle cross section). Chars generated from DAS treated samples (Fig. 5A and B) reproduce the more ordered macropore structure already noted prior the pyrolysis process. The reduction in the amounts of volatile products generated, in comparison with the absence of treatment, may also partly contribute to this result. No evidence is shown of products generated from salt decomposition. On the other hand, the reactions of DAS decomposition are completed for the temperature of 800 K used in the pyrolysis experiments, giving rise to the formation of H_2O , NH_3 and SO_3 [26].

SEM images of chars generated from DAP treated samples (Fig. 6A and C, particle cross section) show that the porous

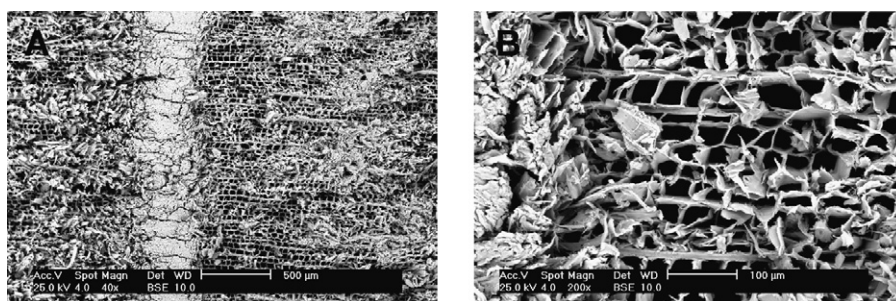


Fig. 2. SEM images of the cross (perpendicular to the trunk fibers) surface of DAS treated wood.

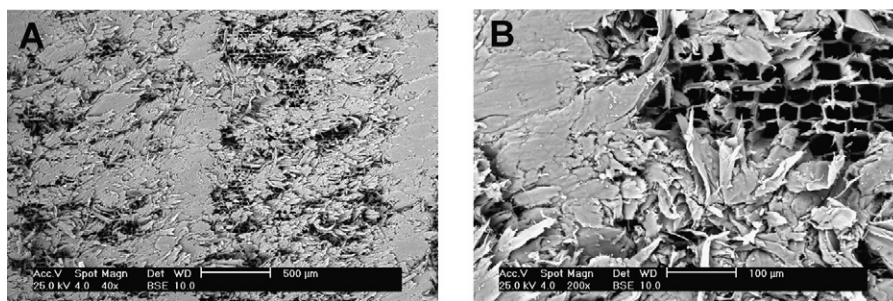


Fig. 3. SEM images of the cross (perpendicular to the trunk fibers) surface of DAP treated wood.

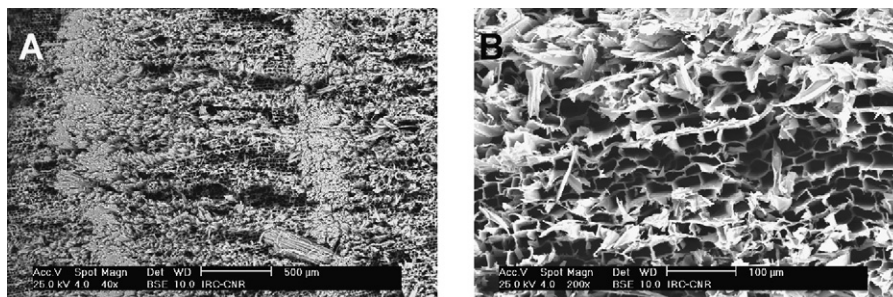


Fig. 4. SEM images of the cross (perpendicular to the trunk fibers) surface of untreated wood char.

structure is collapsed in some zones, probably as a consequence of the attack to the wood structure by the acids formed [26] during the thermal treatment process. At low temperatures (432–482 K) the salt releases NH_3 , leading to the formation of phosphoric acid (H_3PO_4) in the liquid phase. Then the acid is dehydrated, producing pyrophoric acid ($\text{H}_4\text{P}_2\text{O}_7$) which is still a liquid-phase product. At temperatures above 482 K, a slow-rate reaction leads to the formation of phosphorous oxide (P_2O_5), a solid phase product which is preserved in the char structure owing to the relatively mild pyrolysis conditions (800 K) and appears as a coating unevenly distributed especially over the longitudinal surface of the pores (Fig. 6D). Based on the stoichiometry of DAP decomposition, the amount of P_2O_5 formed correspond to about 54% of the added salt mass [26]. Therefore, with reference to the 38% of char formed on a dry wood basis, the char samples used in the thermogravimetric tests include a contribution of 7.11% of P_2O_5 . Given a melting temperature of 842 K and a boiling point of 864 K [27], P_2O_5 is expected to undergo a sublimation process in the last portion of the heating program of the thermogravimetric analysis which foresees a maximum heating temperature of 873 K.

4.2. Kinetic analysis

The simultaneous evaluation of the thermogravimetric curves for the char derived from the untreated (washed) wood has confirmed that a two-step mechanism (devolatilization and combustion) provides accurate predictions with parameters (Table 1) which are roughly the same as those previously determined for Douglas fir wood [10]. Differences can be attributed, for the sample of interest here, to (a) the removal of a large part of alkali metals by hot washing of wood, (b) the possible influences of geographical origin and variety of fir wood (different for the two cases), and (c) the different thermal conditions during pyrolysis (a packed bed in this case and a 4 cm thick wood cylinder in the previous work). However, it is believed that the first issue is predominant as the slightly higher activation energy of the combustion reaction (190 versus 183 kJ/mol) can be plausibly justified by the lack of natural catalysts.

The analysis of the thermogravimetric curves for the chars produced from salt impregnated wood has indicated that a two-step kinetic mechanism produces poor results. Hence, three parallel reactions have been applied and, to facilitate the

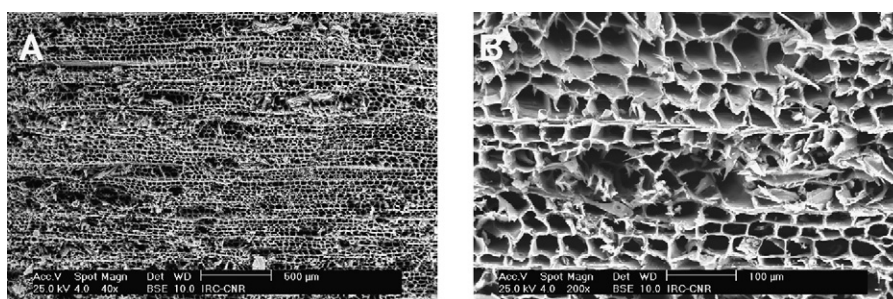


Fig. 5. SEM images of the cross (perpendicular to the trunk fibers) surface of DAS treated wood char.

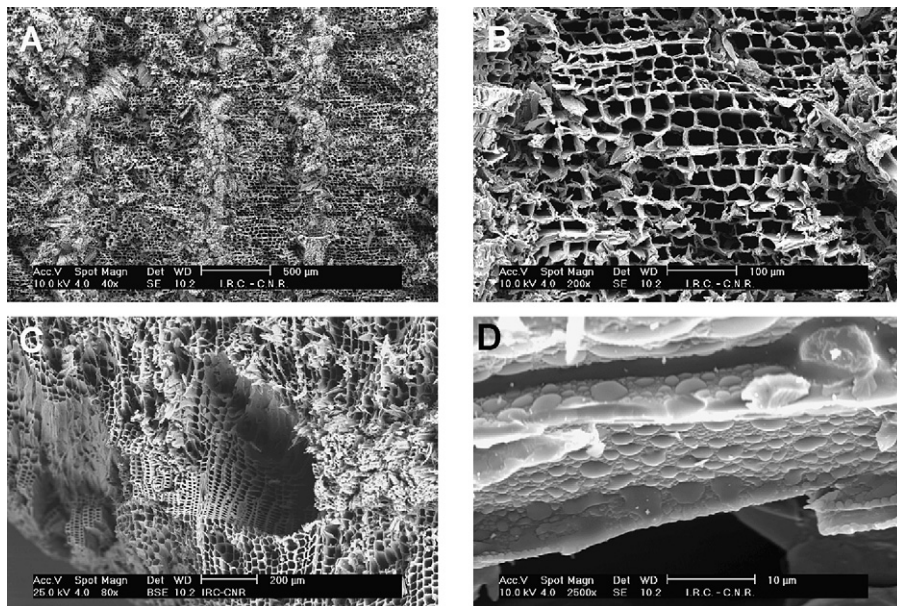


Fig. 6. SEM images of the cross (perpendicular to the trunk fibers), A–C and of the lateral (parallel to the trunk fibers), D, surface of DAP treated wood char.

understanding of salt effects, the same model has also been developed for the chars originated from untreated (washed) wood, although the accuracy level of the predictions is not significantly improved [10]. Furthermore, it should be pointed out that the different characteristics of the weight loss curves give rise to a differentiation in the devolatilization and combustion steps between DAP and DAS treatments so that a specific set of kinetic parameters is needed for each case. The estimated kinetic parameters for devolatilization and combustion and the deviations (definitions as in [10]) between measurements and predictions are listed in Table 2. Examples of the component dynamics for the three cases are shown in Figs. 7–9 for a heating rate of 5 K/min. Comparisons between predictions and measurements, for both integral and differential data and for the various heating rates, are provided in Figs. 10–12. Finally, Table 3 summarizes the main parameters of the curves obtained for the various heating rates (values of the peak rates and corresponding temperatures and mass fractions).

In all cases the agreement between predictions and measurements is good. From the qualitative point of view, the weight loss characteristics remain always the same, that is, a low-temperature shoulder, representative of char devolatilization,

Table 1
Estimated values of kinetic parameters for the oxidation of char produced from Douglas fir wood [10] and fir wood after hot water washing (two-reaction model)

Sample	Hot water washing	No pretreatment
Devolatilization	$E_1 = 114.0$ (kJ/mol)	$E_1 = 121.0$ (kJ/mol)
	$A_1 = 2.42 \times 10^6$ (s^{-1})	$A_1 = 2.72 \times 10^6$ (s^{-1})
	$\nu_1 = 0.185$	$\nu_1 = 0.185$
Combustion	$E_2 = 190.0$ (kJ/mol)	$E_2 = 182.6$ (kJ/mol)
	$A_2 = 1.05 \times 10^{11}$ (s^{-1})	$A_2 = 2.82 \times 10^{10}$ (s^{-1})
	$n_2 = 0.70$	$n_2 = 1.33$
	$\nu_2 = 0.815$	$\nu_2 = 0.815$

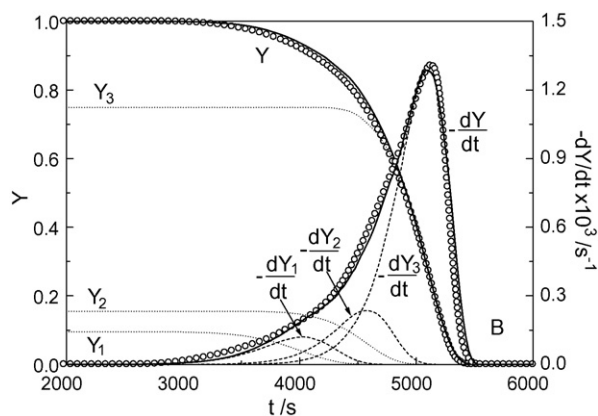


Fig. 7. Mass fraction and time derivative of the mass fraction as functions of time, as measured (symbols) and predicted (lines), and predicted component dynamics for char from untreated (washed) wood and a heating rate of 5 K/min (kinetic constants as in Table 2).

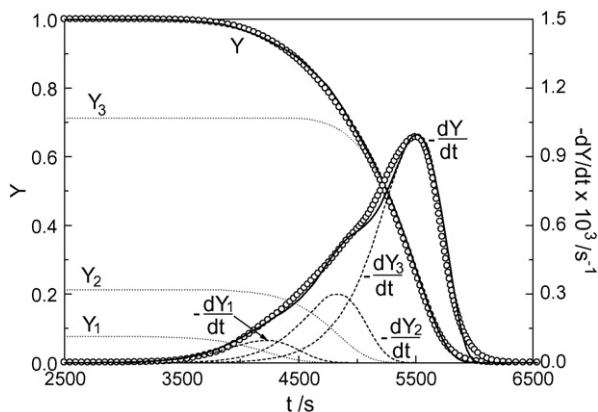


Fig. 8. Mass fraction and time derivative of the mass fraction as functions of time, as measured (symbols) and predicted (lines), and predicted component dynamics for char from diammonium sulphate treated wood and a heating rate of 5 K/min (kinetic constants as in Table 2).

Table 2

Estimated values of kinetic parameters and deviations between measured and predicted curves for the various char samples and heating rates, h

Sample	Untreated	DAS treated	DAP treated
Devolatilization	$E_1 = 135.0$ (kJ/mol) $A_1 = 2.40 \times 10^8$ (s^{-1}) $E_2 = 190.0$ (kJ/mol) $A_2 = 7.80 \times 10^{11}$ (s^{-1}) $n_1 = n_2 = 1.00$	$E_1 = 143.0$ (kJ/mol) $A_1 = 5.50 \times 10^8$ (s^{-1}) $E_2 = 190.0$ (kJ/mol) $A_2 = 2.75 \times 10^{11}$ (s^{-1}) $n_1 = n_2 = 1.00$	$E_1 = 143.0$ (kJ/mol) $A_1 = 3.55 \times 10^8$ (s^{-1}) $n_1 = 1.00$
			$E_2 = 149.0$ (kJ/mol) $A_2 = 4.10 \times 10^7$ (s^{-1}) $n_2 = 1.35$
Combustion	$E_3 = 226.0$ (kJ/mol) $A_3 = 4.10 \times 10^{13}$ (s^{-1}) $n_3 = 0.86$	$E_3 = 200.0$ (kJ/mol) $A_3 = 1.10 \times 10^{11}$ (s^{-1}) $n_3 = 0.86$	$E_3 = 177.0$ (kJ/mol) $A_3 = 4.55 \times 10^8$ (s^{-1}) $n_3 = 1.05$
	Untreated	DAS treated	DAP treated
	$h = 5$ $h = 10$ L/min $h = 15$ L/min	$h = 5$ L/min $h = 10$ L/min $h = 15$ L/min	$h = 5$ L/min $h = 10$ L/min $h = 15$ L/min
ν_1	0.095	0.076	0.085
ν_2	0.155	0.212	0.747
ν_3	0.750	0.712	0.168
devDTG (%)	4.1	3.4	1.9
devTG (%)	1.0	0.7	0.9

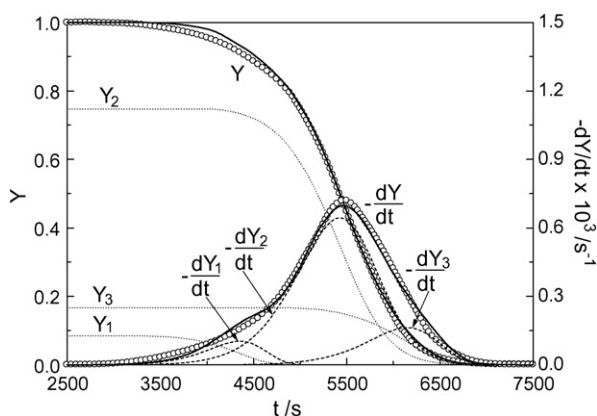


Fig. 9. Mass fraction and time derivative of the mass fraction as functions of time, as measured (symbols) and predicted (lines), and predicted component dynamics for char from diammonium phosphate treated wood and a heating rate of 5 K/min (kinetic constants as in Table 2).

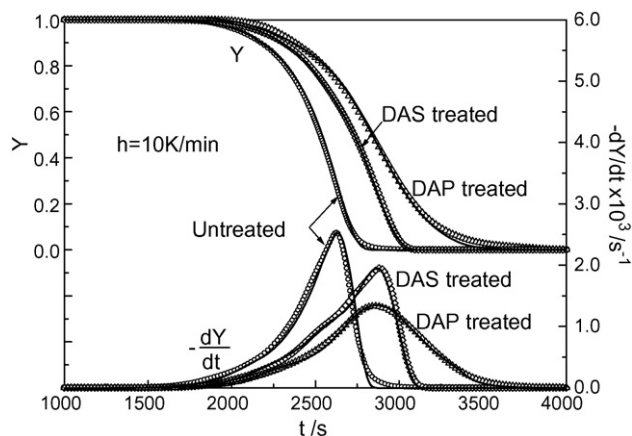


Fig. 11. Mass fraction and time derivative of the mass fraction as functions of time, as measured (symbols) and predicted (lines) for the various samples and a heating rate of 10 K/min (kinetic constants as in Table 2).

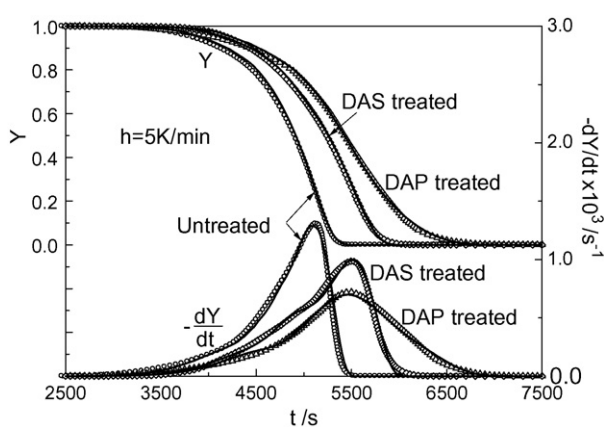


Fig. 10. Mass fraction and time derivative of the mass fraction as functions of time, as measured (symbols) and predicted (lines) for the various samples and a heating rate of 5 K/min (kinetic constants as in Table 2).

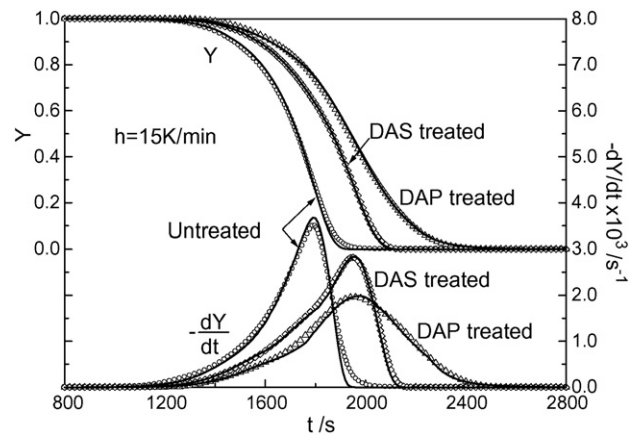


Fig. 12. Mass fraction and time derivative of the mass fraction as functions of time, as measured (symbols) and predicted (lines) for the various samples and a heating rate of 15 K/min (kinetic constants as in Table 2).

Table 3
Values of the peak rates and corresponding temperatures and mass fractions for the various char samples and heating rates, h

Peak variables	Untreated	DAS	DAP
$h = 5 \text{ K/min}$			
$T \text{ (K)}$	739	770	770
Y	0.215	0.236	0.415
$-(dY/dt) \times 10^3 \text{ (s}^{-1}\text{)}$	1.306	0.984	0.679
$h = 10 \text{ K/min}$			
$T \text{ (K)}$	749	789	787
Y	0.275	0.271	0.473
$-(dY/dt) \times 10^3 \text{ (s}^{-1}\text{)}$	2.520	1.917	1.330
$h = 15 \text{ K/min}$			
$T \text{ (K)}$	761	799	798
Y	0.292	0.285	0.491
$-(dY/dt) \times 10^3 \text{ (s}^{-1}\text{)}$	3.503	2.825	1.961

is followed by a peak rate, actually corresponding to combustion (Figs. 10–12). However, for the char obtained from salt impregnated wood, the process becomes much slower, that is, the beginning and especially the completion of the process is delayed with maximum peak rates significantly reduced. The position of the peak rate is delayed of about 30–40 K, depending on the heating rate, for DAP and DAS treated samples (Table 3). The maximum peak rates are reduced by about 24–19% (DAS) and 48–44% (DAP). It is also evident that the mass fractions corresponding to the combustion peak are roughly the same for untreated and DAS treated samples (0.21–0.29, depending on the heating rate), whereas much higher values are observed in the case of DAP treated samples (0.41–0.49). In fact, in this case, the delay in the onset and completion of the reaction process is especially pronounced, as also indicated by the much larger width of the rate curve. These features are also confirmed by the reactivity curves which present large variations especially for conversions above 50% (not shown). For instance, for a heating rate of 5 K/min, the reactivity is reduced by factors from 1.5 to 2 and from 2.5 to 4, for DAS and DAP treatments, respectively, as the conversion varies from 80 to 95%. It can be speculated that the reduction in the char reactivity, in the case of DAS treated samples, is mainly originated by the more ordered structure which is generally associated with a reduced availability of active sites for the oxidation process [7]. For the DAP treated samples, the partial collapse of the porous structure and the presence of phosphorous oxide which, as suggested by previous studies [12,14], may serve as a thermal and oxygen barrier, are certainly factors responsible for the reduction of the char reactivity in air.

The differences in the shape and characteristic parameters of the thermogravimetric curves appear in the kinetic constants of the three-step model developed here. More precisely, for untreated and DAS treated samples, the model consists of two devolatilization and one combustion reactions (Table 2). Component dynamics (Figs. 7 and 8) show a significant overlap between the two devolatilization zones and between the second devolatilization zone and the combustion zone. For DAP treated samples, a single devolatilization reaction is associated

with two combustion reactions (Table 2). In this case, component dynamics (Fig. 9) show a significant overlap between the activity of the two combustion reactions. The description of the combustion peak is characterized by the release of about 75–76 (untreated samples), 71–73 (DAS treated samples) and 75–80 (DAP treated samples)% of volatile matter. Following the similarity in the shape of the DTG curves, the activation energies are about the same (226 and 200 kJ/mol) and the reaction orders coincident (0.86) for untreated and DAS treated samples. The lower activation energy of the DAP treated sample (149 kJ/mol) is accompanied by a higher reaction order (1.35) as a consequence of the slower rates. The first devolatilization reaction deals with 7–10% of volatile matter and the estimated activation energies are comparable for the three cases. However, on the whole, taking into account the contribution of the second reaction, for the untreated and DAS treated samples, devolatilization contributes for about 24–29% of the total volatile produced. On the other hand, an additional combustion reaction, active at high temperatures, should be considered for the DAP treated samples with a contribution of about 13–17%, where about the half (7.11%) is most likely due to the sublimation of P_2O_5 .

5. Conclusions

Significant differences are observed in the shape and characteristic parameters of weight loss curves in air of chars produced from pyrolysis of wood and wood treated with DAP and DAS (5% on a dry wood basis). For the conditions of thermal analysis (heating rates of 5–15 K/min up to 873 K), the onset and completion of the oxidation process are always displaced at higher temperatures (by about 30–40 K) and the peak rate is reduced by about 19–24% (DAS) or 48–44% (DAP), that is, the effects of the two salts are qualitatively similar but those of the DAP treatment are quantitatively stronger. SEM images of char particles show that, compared with untreated samples, the DAS treatment produces a highly ordered macropore structure, owing to the production of lower amounts of volatiles during pyrolysis and to the modifications introduced in the wood structure by salt addition (partial cleaning of the filaments and enlargement of the macropore structure). Chars generated from DAP treated wood present wide zones where the again more ordered porous structure is collapsed. Furthermore, the presence of phosphorous oxide is well evident along the later surface of the pores (salt in wood is well distributed over the cross surface of the particles and occludes, for a large part, the macropores) hindering the diffusion of oxygen towards the active material. These features may explain the changes in the reactivity of chars generated from DAS or DAP treated wood.

A three-reaction model has been applied for the interpretation of the measurements. As a result of the similarity in the shape of the weight loss curves, it consists of two devolatilization reactions and one combustion reaction, with comparable values of activation energies and reaction orders, for untreated and DAS treated samples (differences in the reactivity are taken effectively into account by pre-exponential factors). On the whole, the amount of volatile matter released during the devolatilization stage is about 24–28% and the activation energies are 135

(untreated samples) and 143 kJ/mol (DAS treated samples) for the first reaction and 190 kJ/mol for the second reaction. The corresponding activation energies for the combustion reaction are 226 kJ/mol and 200 kJ/mol, respectively.

Chars from wood treated with DAP present a single devolatilization step with released volatile matter of about 8.5–7% and an activation energy of 143 kJ/mol (as in the case of the DAS treatment). Combustion is described by two reactions, the first corresponding to a high peak of volatile species release (75–80%), followed by a small peak. The reduced reactivity, well evident from the weight loss characteristics when compared with the other two samples, results in a lower activation energy (149 kJ/mol) and a higher reaction order (1.35).

Acknowledgements

This work is part of the EU project HPRN-CT-2002-00197 “Underventilated Compartment Fires” whose partial support is greatly appreciated. The authors also thank Mrs. Clelia Zucchini and Mr. Sabato Russo of Istituto di Ricerche sulla Combustione, CNR (Napoli, IT) for the SEM images of wood and char samples.

References

- [1] C. Di Blasi, *Prog. Energy Combust. Sci.* 19 (1993) 71–104.
- [2] N.M. Laurendeau, *Prog. Energy Combust. Sci.* 4 (1978) 221–270.
- [3] I.W. Smith, *Proceedings of the 19th International Symposium on Combustion*, The Combustion Institute, 1982, pp. 1045–1065.
- [4] L.A. Ruth, *Prog. Energy Combust. Sci.* 24 (1998) 545–564.
- [5] F. Shafizadeh, Y. Sekiguchi, *Combust. Flame* 55 (1984) 171–179.
- [6] T. Kashiwagi, H. Nambu, *Combust. Flame* 88 (1992) 345–368.
- [7] A.M.C. Janse, H.G. de Jonge, W. Prins, W.P.M. van Swaaij, *Ind. Eng. Chem. Res.* 37 (1998) 3909–3918.
- [8] C. Di Blasi, F. Buonanno, C. Branca, *Carbon* 37 (1999) 1227–1238.
- [9] G. Varhegyi, P. Szabo, M.J. Antal, *Energy Fuels* 16 (2002) 724–731.
- [10] C. Branca, C. Di Blasi, *Energy Fuels* 17 (2003) 1609–1615.
- [11] G. Varhegyi, E. Meszaros, M.J. Antal, J. Bourke, E. Jakab, *Ind. Eng. Chem. Res.* 45 (2006) 4962–4970.
- [12] S.L. LeVan, *Chemistry of fire retardancy*, in: R.M. Rowell (Ed.), *The chemistry of solid wood*. *Advances in Chemistry series 207*, ACS, Washington DC, 1984, pp. 531–574.
- [13] R. Kozłowski, M. Władysław-Przybyłank, *Natural polymers, wood and lignocellulosic materials*, in: A.R. Horrocks, D. Price (Eds.), *Fire Retardant Materials*, Woodhead Publishing Limited, 2001, pp. 293–317.
- [14] B.K. Kandola, A.R. Horrocks, D. Price, G.V. Coleman, *J.M.S. Rev. Macromol. Chem. Phys.* C36 (1996) 721–794.
- [15] F. Shafizadeh, A.G.W. Bradbury, W.F. DeGroot, T.W. Aanerud, *Ind. Eng. Chem. Rod. Res. Dev.* 21 (1982) 97–101.
- [16] C. Branca, P. Giudicianni, C. Di Blasi, *Ind. Eng. Chem. Res.* 42 (2003) 3190–3202.
- [17] C. Di Blasi, C. Branca, A. Galgano, *Ind. Eng. Chem. Res.* 46 (2007) 430–438.
- [18] C. Di Blasi, C. Branca, G. D’Errico, *Thermochim. Acta* 364 (2000) 133–142.
- [19] C. Di Blasi, C. Branca, *Ind. Eng. Chem. Res.* 40 (2001) 5547–5556.
- [20] C. Branca, C. Di Blasi, H. Horacek, *Ind. Eng. Chem. Res.* 41 (2002) 2104–2114.
- [21] C. Branca, C. Di Blasi, *Fuel* 83 (2004) 81–87.
- [22] M.G. Gronli, G. Varhegyi, C. Di Blasi, *Ind. Eng. Chem. Res.* 41 (2002) 4201–4208.
- [23] G. Varhegyi, M.G. Gronli, C. Di Blasi, *Ind. Eng. Chem. Res.* 43 (2004) 2356–2367.
- [24] J.A. Conesa, A. Marcilla, J.A. Caballero, R. Font, *J. Anal. Appl. Pyrolysis* 58–59 (2001) 617–633.
- [25] P. Alvarez, C. Blanco, R. Santamaria, M. Granda, *J. Anal. Appl. Pyrolysis* 72 (2004) 131–139.
- [26] M. Statheropoulos, S.A. Kyriakou, *Anal. Chim. Acta* 409 (2000) 203–214.
- [27] R.H. Perry, D.W. Green, J.O. Maloney (Eds.), *Perry’s Chemical Engineering Handbook*, Sixth Edition International Student Edition, McGraw-Hill Book Company, New York, 1984, p. 121.